Neodymium Nitrate and Yttrium Nitrate as Environmentally Friendly Corrosion Inhibitors for Carbon Steel Used in Petroleum Equipments

A. M. El-desoky[*a], A. S. Fouda[b], and D. M. Eid[c]

[*a] Engineering Chemistry Department, High Institute of Engineering &Technology (New Damietta), Egypt and Al-Qunfudah Center for Scientific Research (QCSR), Chemistry Department, Al-Qunfudah University College, Umm Al-Qura University, KSA.
email: a.m.eldesoky79@hotmail.com
[b] Department of Chemistry, Faculty of Science, El-Mansoura University, El-Mansoura-35516, Egypt
[c] Nuclear Materials Authority, Egypt and TA in Qatar University, Qatar.

Abstract- Neodymium nitrate and Yttrium nitrate as environmentally friendly corrosion inhibitors for carbon steel used in Petroleum Equipments using electrochemical techniques [potentiodynamic polarization, electrochemical impedance spectroscopy, and electrochemical frequency modulation]. The adsorption of these compounds on carbon steel surface was found to be of neither a typical physisorption nor a typical chemisorption mode. Increase in temperature increases corrosion rate but decreases inhibition efficiency. The thermodynamic functions of activation have been evaluated. The polarization measurements indicated that the inhibitors are of mixed type. The adsorption of these compounds was found to obey Langmuir's adsorption isotherm. The analysis of SEM and EDS confirmed the formation of precipitates of these compounds on Carbon steel surface, which reduced the overall corrosion reaction.

Index Terms— Langmuir's isotherm, EFM, EIS, SEM–EDX; Environmentally

1 Introduction

Carbon steel used in most industries because of its low cost and availability for manufacture of reaction vessels such as cooling towers reservoirs, pipelines, boilers, drums heat exchangers, tanks, etc. Carbon steel structure is highly susceptible to corrosion and its protection costs billions of dollars annually. Various additives are used to protect iron and its alloy against corrosive attack. It is well known that some rare earth form insoluble hydroxides which enable them to be used as cathodic inhibitors. Neodymium nitrate and Yttrium nitrate have a low toxicity and their ingestion or inhalation has not been considered harmful to health [1], whilst the toxic effects of their oxides are similar to those produced by sodium chloride. Furthermore, Neodymium nitrate and Yttrium nitrate can be considered as economically competitive products [2] because, as elements, some of them are relatively abundant in nature. Cerium, for instance, is as plentiful as copper [3]. Production of rare earth has shown a continuous increase in recent years. Taking all these facts into account, it is reasonable to use this family of compounds as save corrosion inhibitors. There are several papers in the literature dealing with the use of some rare earth elements as corrosion inhibitors for several metals and alloys such as zinc [4–6], mild steels [7], and stainless steels [8–14]. Several researches were found in the literature about the use of inhibitors for metals and alloys in sea water [15–17].

The purpose of this paper is to compare the corrosion inhibition data derived from EFM with that obtained from Tafel extrapolation and EIS techniques. SEM and EDX examination of the carbon steel in 0.5 M HCl surface revealed that these compounds prevented carbon steel in 0.5 M HCl from corrosion by adsorption on its surface to form a protective film and acts as a barrier to corrosive media.

2 Experimental Details

2.1 Composition of Material Samples

TABLE 1
CHEMICAL COMPOSITION (WEIGHT %) OF THE CARBON STEEL

Element	C	Mn	P	Si	Fe
Weight (%)	0.200	0.350	0.024	0.003	rest

2.2 Chemicals and Solutions

2.2.1 Chemicals

a- Hydrochloric Acid (BDH grade)

b- Neodymium nitrate and yttrium nitrate (BDH grade) purchased from Alfa Aesar, Ajohnson Matthy Company, the lanthanide nitrates [Neodymium (III) nitrate $Nd(NO_3)_3$ with mol. weight = 438.34 and Yterbium(III) nitrate $Yb(NO_3)_3$ with mol. Weight 467.15]

2.3 Electrochemical Measurements

The experiments were carried out potentiodynamically in a thermostated three electrode cell. Platinum foil was used as counter electrode and a saturated calomel electrode (SCE) coupled to a fine Lug-

gin capillary as the reference electrode. The working electrode was in the form of a square cut from C-steel under investigation and was embedded in a Teflon rod with an exposed area of 1 cm^2. This electrode was immersed in 100 ml of a test solution for 30 min until a steady state open-circuit potential (Eocp) was attained. Potentiodynamic polarization was conducted in an electrochemical system (Gamry framework instruments version 3.20) which comprises a PCI/300 potentiostat, controlled by a computer recorded and stored the data. The potentiodynamic curves were recorded by changing the electrode potential from -1.0 to 0.0 V versus SCE with scan rate of 5 mV/s. All experiments were carried out in freshly prepared solution at constant temperature (25 ±1 ^oC) using a thermostat. %IE and the degree of surface coverage (θ) were defined as:

$$\% IE = \theta \times 100 = [(i_{corr} - i_{corr(inh)}) / i_{corr}] \times 100 \quad (1)$$

where i_{corr} and $_{icorr(inh)}$ are the uninhibited and inhibited corrosion current density values, respectively, determined by extrapolation of Tafel lines.

The electrochemical impedance spectroscopy (EIS) spectra were recorded at open circuit potential (OCP) after immersion the electrode for 15 min in the test solution. The ac signal was 5 mV peak to peak and the frequency range studied was between 100 kHz and 0.2 Hz. All Electrochemical impedance experiments were carried out using Potentiostat/Galvanostat/Zra analyzer (Gamry PCI 300/4). A personal computer with EIS300 software and Echem Analyst 5.21 was used for data fitting and calculating.

The inhibition efficiency (% IE) and the surface coverage (θ) of the used inhibitors obtained from the impedance measurements were calculated by applying the following relations:

$$\% IE = \theta \times 100 = [1-(R°ct/Rct)] \quad (2)$$

Where, Roct and Rct are the charge transfer resistance in the absence and presence of inhibitor, respectively.

EFM experiments were performed with applying potential perturbation signal with amplitude 10 mV with two sine waves of 2 and 5 Hz. The choice for the frequencies of 2 and 5Hz was based on three arguments [18]. The larger peaks were used to calculate the corrosion current density (i_{corr}), the Tafel slopes (βc and βa) and the causality factors CF2 and CF3 [19]. All electrochemical experiments were carried out using Gamry instrument PCI300/4 Potentiostat/Galvanostat/Zra analyzer, DC105 Corrosion software, EIS 300 Electrochemical Impedance Spectroscopy software, EFM 140 Electrochemical Frequency Modulation software and Echem Analyst 5.5 for results plotting, graphing, data fitting and calculating.

2.4 SEM-EDX Measurement

The carbon steel surface was prepared by keeping the specimens for 3 days immersion in 0.5 M HCl in the presence and absence of optimum concentrations of Neodymium nitrate and Yttrium nitrate compounds, after abraded using different emery papers up to 1200 grit size. Then, after this immersion time, the specimens were washed gently with distilled water, carefully dried and mounted into the spectrometer without any further treatment. The corroded C-steel surfaces were examined using an X-ray diffractometer Philips (pw-1390) with Cu-tube (Cu Ka_1, l = 1.54051 A°), a scanning electron microscope (SEM, JOEL, JSM-T20, Japan).

3. Results and Discussion

3.1Potentiodynamic Polarization Measurements

Fig. (1) shows the potentiodynamic polarization curves for carbon steel without and with different concentrations of $Yb(NO_3)_3$ at 25 ^oC. Similar curves were obtained for $Nd(NO_3)_3$ compound. The obtained electrochemical parameters; cathodic (βc) and anodic (βa) Tafel slopes, corrosion potential (E_{corr}), and corrosion current density (i_{corr}), were obtained and listed in Table. (2). Table. (2) shows that icorr decreases by adding the rare earth compounds and by increasing their concentration. In addition, Ecorr does not change obviously. Also βa and βc do not change markedly, which indicates that the mechanism of the corrosion reaction of carbon steel does not change. Fig. (1) clearly shows that both anodic and cathodic reactions are inhibited, which indicates that investigated compounds act as mixed-type inhibitors [20-21]. The inhibition achieved by these compounds decreases in the following order: $Yb(NO_3)_3 > Nd(NO_3)_3$

Also, the results of θ and % IE where calculated using icorr values. The percentage inhibition efficiencies (% IE) calculated from icorr of the investigated compounds are given in Table (2). An inspection of the results obtained from this Table reveals that, the presence of different concentrations of the additives reduces the anodic and cathodic current densities and the polarization resistance. This indicates that the inhibiting effects of the investigated compounds. The order of decreasing inhibition efficiency from icorr is: $Yb(NO_3)_3 > Nd(NO_3)_3$.

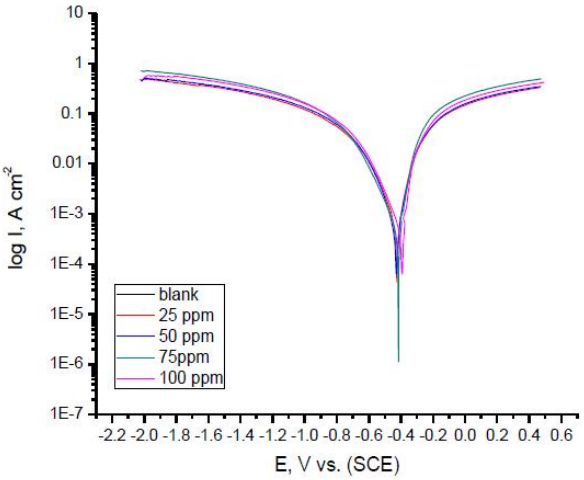

Fig. (1): Potentiodynamic polarization curves for the corrosion of C-steel in 0.5 M HCl in the absence and presence of various concentrations of $Yb(NO_3)_3$ at 25°C

TABLE (2)

EFFECT OF CONCENTRATIONS OF THE INVESTIGATED COMPOUNDS ON THE FREE CORROSION POTENTIAL ($E_{CORR.}$), CORROSION CURRENT DENSITY ($I_{CORR.}$), TAFEL SLOPES (BA&BC), DEGREE OF SURFACE COVERAGE (θ) AND INHIBITION EFFICIENCY (% IE) FOR CARBON STEEL IN 0.5 M HCL AT 30°C.

Conc., ppm		- $E_{corr.}$ mV(vs SCE)	$I_{corr.}$ mA cm^{-2}	β_c mV dec^{-1}	β_a mV dec^{-1}	Θ	% IE
0.0		533	21.40	551	520	-	-
$Yb(NO_3)_3$	25	425	7.31	138	80	0.658	65.8
	50	428	5.43	126	80	0.746	74.6
	75	415	4.82	149	62	0.775	77.5
	100	394	4.28	132	47	0.800	80.0
$Nd(NO_3)_3$	25	386	9.26	169	74	0.567	56.7
	50	398	7.56	148	55	0.647	64.7
	75	383	5.69	169	65	0.734	73.4
	100	410	4.69	144	63	0.781	78.1

3.1.2 Adsorption Isotherm

The adsorption isotherms are considered to describe the interactions of the inhibitor molecule with the active sites on the metal surface [22]. Attempts were made to fit θ values to various isotherms including Frumkin, Langmuir, Temkin, and Freundlich. The results were best fitted by far by the Langmuir adsorption isotherm which has the following equation [23-24]:

$$C/\theta = 1/K_{ads} + C \quad (3)$$

where C is the concentration of lanthanides; Kads is the adsorptive equilibrium constant; and θ is the surface coverage of lanthanides on carbon steel, which can be calculated by the ratio of IE/100 for different lanthanides concentration [45]. Figs. (2-3) show the straight lines of θ vs. C at T_1 (25 °C) and T2 (45 °C), respectively. The linear correlation coefficients (0.9968) (0.9988), at 25 °C and (0.998), (0.998) at 45°C are almost equal to 1 and the slopes (1.13), (1.13) at 25 °C and (1.19), (1.20) at 45 °C are close to 1, which confirms the assumption that the adsorption of lanthanide compounds on the carbon steel surface obeys Langmuir adsorption isotherm. The adsorptive equilibrium constants at T_1 (25 °C) namely K_1 are (66.71), (84.82) and T_2 (45 °C), namely K_2 are (52.44) (70.33) M-1, respectively. The value of K_1 is higher than that of K_2, which implies that the high temperature does not benefit the strong adsorption of lanthanides on the carbon steel surface. Thus, for the low concentration of lanthanides, the higher inhibition efficiency at T1(25 °C) when compared to that at T_2 (45 °C) can be well understood.

Moreover, the adsorption heat can be calculated according to the van't Hoff equation [26]:

$$\ln K_{ads} = \Delta H^0_{ads}/RT + \text{Const} \quad (4)$$

That is:

$$\ln(K_{2ads}/K_{1ads}) = -\Delta H^0_{ads}/R(1/T_{2-1}/T_1) \quad (5)$$

where ΔH° is the adsorption heat, R is the gas constant, T is the absolute temperature, K_1 and K_2 are the adsorptive equilibrium constants at T_1 (25°C) and T_2 (45°C), respectively. In consideration that the experiments precede at the standard pressure and the solution concentrations are not very high, which are close to the standard condition, the calculated adsorption heat thus can be approximately regarded as the standard adsorption heat ΔH°_{ads}. The negative values of ΔH° (Table 4.5) reflect the exothermic behavior of the adsorption of lanthanides on the carbon steel surface. The standard adsorption free energy (ΔG°_{ads}) can be obtained according to the following equation [27-28]

$$K_{ads} = 1/55.5 \exp(-\Delta G^\circ ads/RT) \quad (6)$$

The negative values of ΔG^0_{ads} (Table 3) suggest that the adsorption of lanthanides on the carbon steel surface is spontaneous. Generally, the values of ΔG°ads around or less than -20 kJ mol^{-1} are associated with the electrostatic interaction between charged molecules and the charged metal surface (physisorption); while those around or higher than -40 kJ mol^{-1} mean charge sharing or transfer from the inhibitor molecules to the metal surface to form a coordinate type of metal bond (chemisorption). The ΔG^0_{ads} values listed in Table (3) are around -20 kJ mol^{-1}, which means that the absorption of lanthanide compounds on the carbon steel surface belongs to the physisorption and the adsorptive film has an electrostatic char-

acter [29-30]. Finally, the standard adsorption entropy ΔS°ads can be calculated by the following Eq:

$$\Delta S^\circ_{ads} = (\Delta H^\circ_{ads} - \Delta G^\circ_{ads}) / T \quad (7)$$

The (ΔS°_{ads}) values (Table 3) are positive, which are opposite to the usual expectation that the adsorption is an exothermic process and always accompanied by a decrease of entropy. The reason can be explained as follows: the adsorption of lanthanides inhibitor molecules from the aqueous solution can be regarded as a quasi-substitution process between the lanthanides compound in the aqueous phase and water molecules at the electrode surface [$H_2O_{(ads)}$] [31-34]. In this situation, the adsorption of lanthanides is accompanied by the desorption of water molecules from the electrode surface. Thus, while the adsorption process for the inhibitor is believed to be exothermic and associated with a decrease in entropy of the solute, the opposite is true for the solvent [35]. The thermodynamic values obtained are the algebraic sum of the adsorption of lanthanides inhibitor molecules and the desorption of water molecules. Therefore, the gain in entropy is attributed to the increase in solvent entropy. The positive values of (ΔS^0_{ads}) suggest that the adsorption process is accompanied by an increase in entropy, which is the driving force for the adsorption of lanthanides on the Carbon steel surface. Table (3) lists all the above calculated thermodynamic parameters.

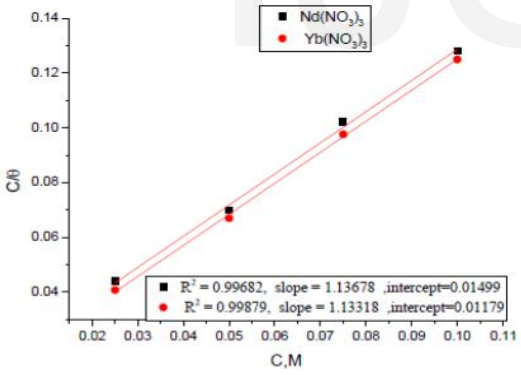

Fig. (2): Langmuir adsorption isotherm plotted as (C/θ) vs. C of lanthanide compounds for the corrosion of carbon steel in 0.5 M HCl at 25°C

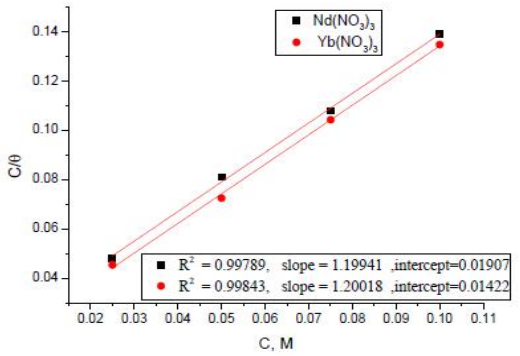

Fig. (3): Langmuir adsorption isotherm plotted as (C/θ) vs. C of lanthanide compounds for the corrosion of carbon steel in 0.5 M HCl at 45°C

TABLE 3

SOME PARAMETERS FROM LANGMUIR ISOTHERM MODEL FOR CARBON STEEL IN 0.5 M HCL FOR LANTHANIDE COMPOUNDS.

Compounds	Temp., K	K_{ads} M^{-1}	$-\Delta G^\circ_{ads}$ kJ mol^{-1}	$-\Delta H^\circ_{ads}$ kJ mol^{-1}	ΔS°_{ads} J mol^{-1}k^{-1}
$Nd(NO_3)_3$	298	66.71	20.36	9.48	36.50
	318	52.44	21.09		
$Yb(NO_3)_3$	298	84.82	20.96	7.38	45.56
	318	70.33	21.87		

3.1.3 Effect of Temperature

The importance of temperature variation in corrosion study involving the use of inhibitors is to determine the mode of inhibitor adsorption on the metal surface. Recently, the use of two temperatures to establish the mode of inhibitor adsorption on a metal surface has been reported and has been found to be adequate [36-37]. Thus, the influence of temperature on the corrosion behavior of carbon steel in 0.5 M HCl in the absence and presence of lanthanides were investigated by hydrogen evolution method at 25 and 45°C. Therefore, in examining the effect of temperature on the corrosion process, the apparent activation energies (Ea) were calculated from the Arrhenius equation [38]

$$\text{Log } (\rho_2/\rho_1) = (Ea/2.303R)\,(1/T_{1\text{-}1}/T_2) \quad (8)$$

where ρ_2 and ρ_1 are the corrosion rates at temperature T_1 and T_2 respectively. An estimate of heat of adsorption was obtained from the trend of surface coverage with temperature as follows [39]:

$$Q_{ads} = 2.303R\,[\log(\theta_2/1\text{-}\theta_2) - \log(\theta_1/1\text{-}\theta_1)]x(T_1xT_2/T_1\text{-}T_2)\ \text{kJmol}^{-1} \quad (9)$$

where θ_1 and θ_2 are the degrees of surface coverage at temperatures T_1 and T_2, the calculated values for both parameters are given in Tables (4-5). Increased activation energy (Ea) in inhibited solutions compared to the blank suggests that the inhibitor is physically adsorbed on the corroding metal surface while either unchanged or lower Ea in the presence of inhibitor suggest chemisorptions. It is seen from Tables (4-5) that Ea values were higher in the presence of the additives compared to that in their absence hence leading to reduction in the corrosion rates. It has been suggested that adsorption of an organic inhibitor can affect the corrosion rate by either decreasing the available reaction area (geometric blocking effect) or by modifying the activation energy of the anodic or cathodic reactions occurring in the inhibitor-free surface in the course of the inhibited corrosion process [40]. The Ea values support the earlier proposed physisorption mechanism. Hence, corrosion inhibition is assumed to occur primarily through physical adsorption on the carbon steel surface, giving rise to the deactivation of these surfaces to hydrogen atom recombination.

Similar results have been reported in earlier publications [41]. The negative Qads values indicate that the degree of surface coverage decreased with rise in temperature, supporting the earlier proposed physisorption mechanism [42].

TABLE 4

CALCULATED VALUES OF ACTIVATION ENERGY (EA) AND HEAT OF ADSORPTION (Q_{ADS}) FOR CARBON STEEL IN 0.5 M HCL SOLUTIONS CONTAINING VARIOUS CONCENTRATIONS OF THE $Nd(NO_3)_3$ AT 25 AND 45°C OBTAINED FROM POTENTIODYNAMIC POLARIZATION MEASUREMENTS

Conc., ppm		E_a kJ mol^{-1}	$-Q_{ads}$ kJ mol^{-1}
0.5 M HCl		2	
$Nd(NO_3)_3$	25	6.1	7.5
	50	7.3	8.6
	75	9.4	10.5
	100	11.8	13.1

TABLE 5

CALCULATED VALUES OF ACTIVATION ENERGY (EA) AND HEAT OF ADSORPTION (Q ADS) FOR CARBON STEEL IN 0.5 M HCL SOLUTIONS CONTAINING VARIOUS CONCENTRATIONS OF THE $Yb(NO_3)_3$ AT 25 AND 45° C OBTAINED FROM POTENTIODYNAMIC POLARIZATION MEASUREMENTS

Conc., ppm		E_a (kJmol^{-1})	$-Q_{ads}$ (kJmol^{-1})
0.5 M HCl		2	----
$Yb(NO_3)_3$	25	8.4	10.1
	50	9.8	10.9
	75	10.9	12.1
	100	12.0	13.0

3.2 Electrochemical Impedance Spectroscopy (EIS)

The corrosion of carbon steel in 0.5 M HCl in the presence of the investigated compounds was investigated by EIS method at 25 °C after 30 min immersion. Nyquist plots in the absence and presence of investigated compound $Yb(NO_3)_3$ are presented in Fig. (4). Similar curves were obtained for other inhibitor. It is apparent that all Nyquist plots show a single capacitive loop, both in uninhibited and inhibited solutions. The impedance data of carbon steel in 0.5 M HCl are analyzed in terms of an equivalent circuit model Fig. (5) which includes the solution resistance Rs and the double layer capacitance Cdl which is placed in parallel to the charge transfer resistance Rct [43] due to the charge transfer reaction. For the Nyquist plots it is obvious that low frequency data are on the right side of the plot and higher frequency data are on the left. This is true for EIS data where impedance usually falls as frequency rises (this is not true for all circuits). The capacity of double layer (Cdl) can be calculated from the following equation:

$$C_{dl} = \frac{1}{2\pi f_{max} R_{ct}} \quad (10)$$

where f max is maximum frequency. The parameters obtained from impedance measurements are given in Table (6). It can see from Table (6) that the values of charge transfer resistance Rct increase with inhibitor concentration [44]. In the case of impedance studies, % IE increases with inhibitor concentration in the presence of investigated inhibitors and the % IE of these investigated inhibitors is as follows:

$$Yb(NO_3)_3 > Nd(NO_3)_3$$

The impedance study confirms the inhibiting characters of these compounds obtained from potentiodynamic polarization. It is also noted that the (Cdl) values tend to decrease when the concentration of these compounds increases. This decrease in (Cdl), which can result from a decrease in local dielectric constant and/or an increase in the thickness of the electrical double layer, suggests that these compounds molecules function by adsorption at the metal/solution interface [45]. The inhibiting effect of these compounds can be attributed to their parallel adsorption at the metal solution interface. The parallel adsorption is owing to the presence of one or more active center for adsorption.

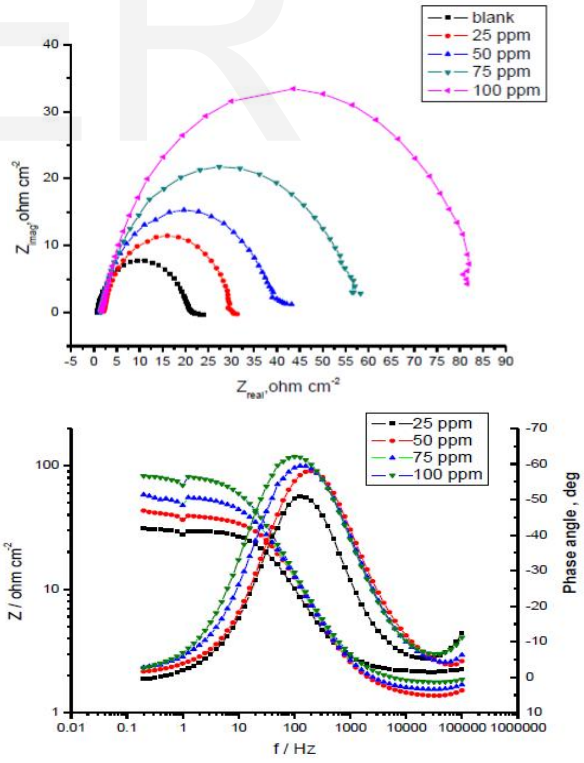

Fig. (4). The Nyquist (a) and Bode (b) plots for corrosion of C-steel in 0.5 M HCl in the absence and presence of different concentrations of $Yb(NO_3)_3$ at 25°C.

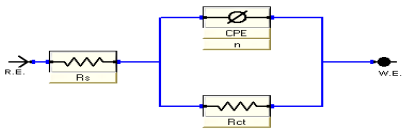

Fig. (5): Equivalent circuit model used to fit the impedance spectra

TABLE 6

ELECTROCHEMICAL KINETIC PARAMETERS OBTAINED FROM EIS TECHNIQUE FOR THE CORROSION OF CARBON STEEL IN 0.5 M HCL AT DIFFERENT CONCENTRATIONS OF INVESTIGATED INHIBITORS AT 25 °C.

Compounds	Concentration, M	C_{dl}, μF cm^{-2}	R_{ct}, ohm cm^2	θ	%IE
Blank	0.5 M HCl	97.88	18.90	----	----
$Yb(NO_3)_3$	25	1.74	29.44	0.358	35.8
	50	1.87	41.28	0.542	54.2
	75	1.77	67.85	0.721	72.1
	100	1.75	123.3	0.847	84.7
$Nd(NO_3)_3$	25	18.3	28.04	0.326	32.6
	50	14.6	38.72	0.512	51.2
	75	16.1	53.98	0.65	65.0
	100	15.5	80.63	0.766	76.6

3.3 Electrochemical Frequency Modulation Technique (EFM)

EFM is a nondestructive corrosion measurement technique that can directly and quickly determine the corrosion current value without prior knowledge of Tafel slopes, and with only a small polarizing signal. These advantages of EFM technique make it an ideal candidate for online corrosion monitoring [46]. The great strength of the EFM is the causality factors which serve as an internal check on the validity of EFM measurement. The causality factors CF-2 and CF-3 are calculated from the frequency spectrum of the current responses. Figs (6) shows the frequency spectrum of the current response of carbon steel in 0.5 M HCl, contains not only the input frequencies, but also contains frequency components which are the sum, difference, and multiples of the two input frequencies. The EFM intermodulation spectrums of carbon steel in 0.5 M HCl acid solution containing (25 ppm-100 ppm) of the studied inhibitors are shown in Fig (6). Similar results were recorded for the other concentrations of the investigated compound (not shown). The harmonic and intermodulation peaks are clearly visible and are much larger than the background noise. The two large peaks, with amplitude of about 200 μA, are the response to the 40 and 100 mHz (2 and 5 Hz) excitation frequencies. It is important to note that between the peaks there is nearly no current response (<100 nA). The experimental EFM data were treated using two different models: complete diffusion control of the cathodic reaction and the "activation" model. For the latter, a set of three non-linear equations had been solved, assuming that the corrosion potential does not change due to the polarization of the working electrode [47]. The larger peaks were used to calculate the corrosion current density (i_{corr}), the Tafel slopes (βc and βa) and the causality factors (CF-2 and CF-3). These electrochemical parameters were simultaneously determined by Gamry EFM140 software, and listed in Table (7). The data presented in Table (7) obviously show that, the addition of any one of tested compounds at a given concentration to the acidic solution decreases the corrosion current density, indicating that these compounds inhibit the corrosion of c- steel in 0.5 M HCl through adsorption. The causality factors obtained under different experimental conditions are approximately equal to the theoretical values (2 and 3) indicating that the measured data are verified and of good quality [48]. The inhibition efficiencies IE EFM % increase by increasing the studied inhibitor concentrations and was calculated as follows:

$$\% IE_{EFM}=[(1-i_{corr}/i_{ocorr})]x100 \quad (11)$$

Where iocorr and icorr are corrosion current densities in the absence and presence of inhibitor, respectively. The inhibition sufficiency obtained from this method is in the order: $Yb(NO_3)_3$ > Nd $(NO_3)_3$.

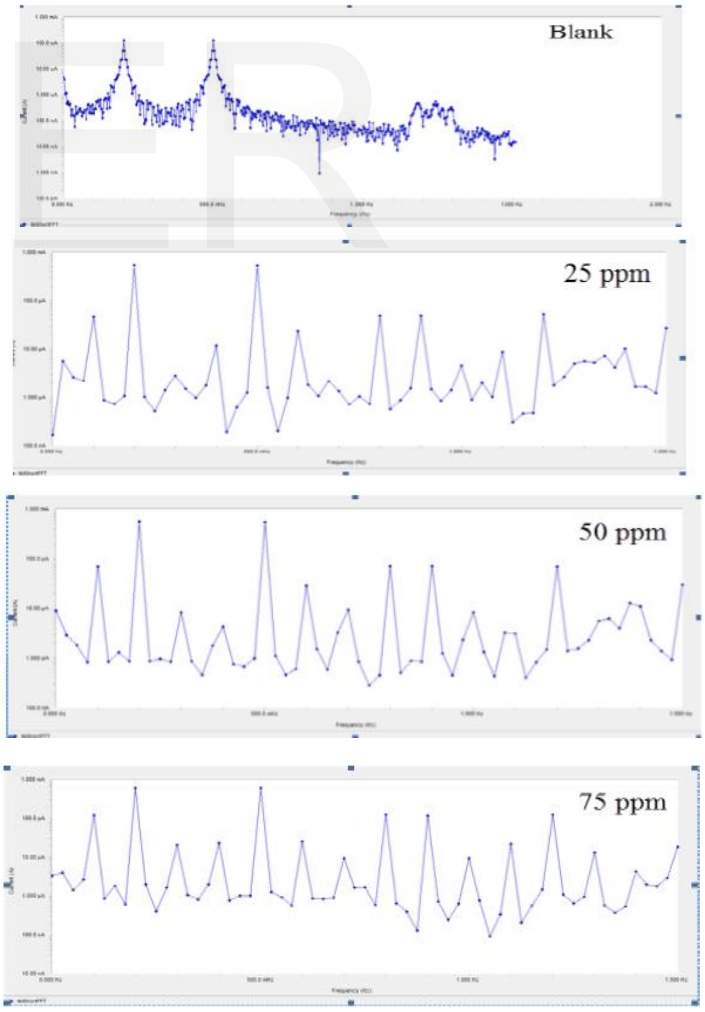

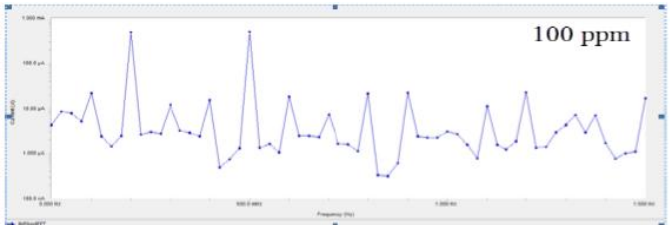

Fig. (6): EFM spectra Carbon steel in 1M HCl in the absence and presence of different concentrations of $Yb(NO_3)_3$ at 25°C.

TABLE 7

ELECTROCHEMICAL KINETIC PARAMETERS OBTAINED FROM EFM TECHNIQUE FOR THE CORROSION OF CARBON STEEL IN 0.5 M HCL AT DIFFERENT CONCENTRATIONS OF INVESTIGATED INHIBITORS AT 25 °C.

Compounds	Conc.	$i_{corr.}$ $\mu A\ cm^{-2}$	β_c, $mV\ dec^{-1}$	β_a, $mV\ dec^{-1}$	CF(2)	CF(3)	θ	% IE
Blank	0.5 M HCl	812.2	409.8	431.8	1.95	2.99	-	-
$Yb(NO_3)_3$	25 ppm	305.8	40.24	34.8	1.55	2.17	0.623	62.3
	50 ppm	263.3	30.8	29.24	1.62	2.84	0.676	67.6
	75ppm	227.	24.31	23.44	2.42	3.22	0.720	72.0
	100ppm	175.3	95.9	87.9	2.04	3.01	0.784	78.4
$Nd(NO_3)_3$	25 ppm	312.6	38.37	38.03	2.05	2.80	0.615	61.5
	50 ppm	277.2	32.9	31.8	1.41	2.39	0.659	65.9
	75ppm	238.1	26.25	25.25	1.90	2.64	0.707	70.7
	100ppm	216.1	22.6	21.57	1.55	2.71	0.734	73.4

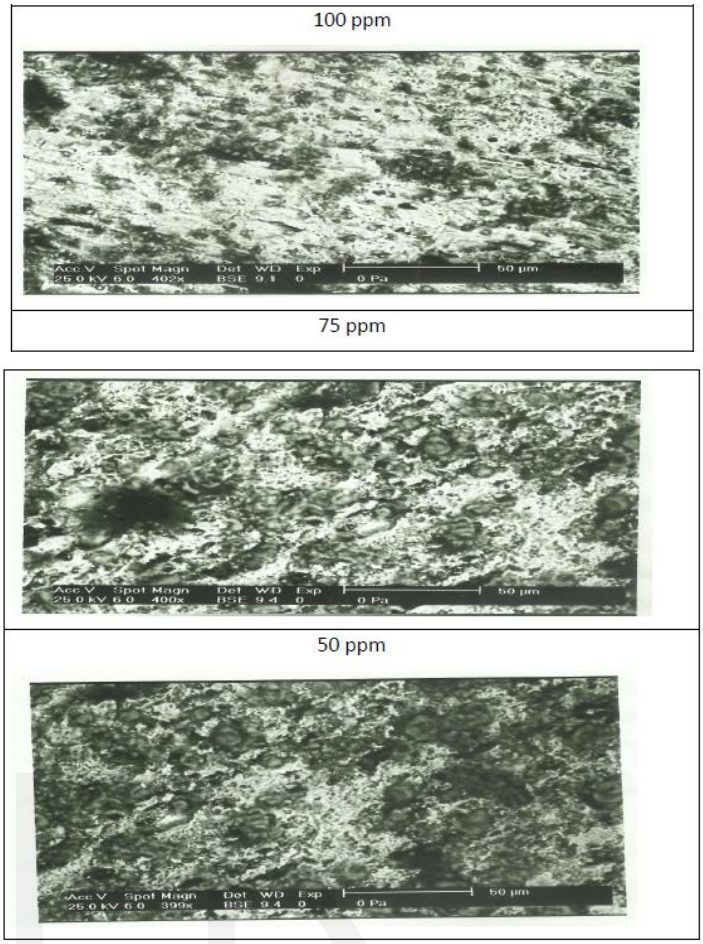

Fig. (7): SEM spectrum of carbon steel before and after immersion for 15 h in 0.5M HCl solution without and with different concentrations of $Nd(NO_3)_3$.

3.5- Scanning Electron Microscopy (SEM) Studies

Figure (7-8) represents the micrography obtained for carbon steel samples in presence and in absence of different concentrations of compounds after exposure for 15 hours' immersion. It is clear that carbon steel surfaces suffer from severe corrosion attack in the blank sample. It is important to stress out that when the compound is present in the solution, the morphology of carbon steel surfaces is quite different from the previous one, and the specimen surfaces were smoother. We noted the formation of a film which is distributed in a random way on the whole surface of the carbon steel. This may be interpreted as due to the adsorption of the rare earth compounds on the carbon steel surface incorporating into the passive film in order to block the active site present on the carbon steel surface. Or due to the involvement of inhibitor molecules in the interaction with the reaction sites of carbon steel surface, resulting in a decrease in the contact between carbon steel and the aggressive medium and sequentially exhibited excellent inhibition effect [49,50]

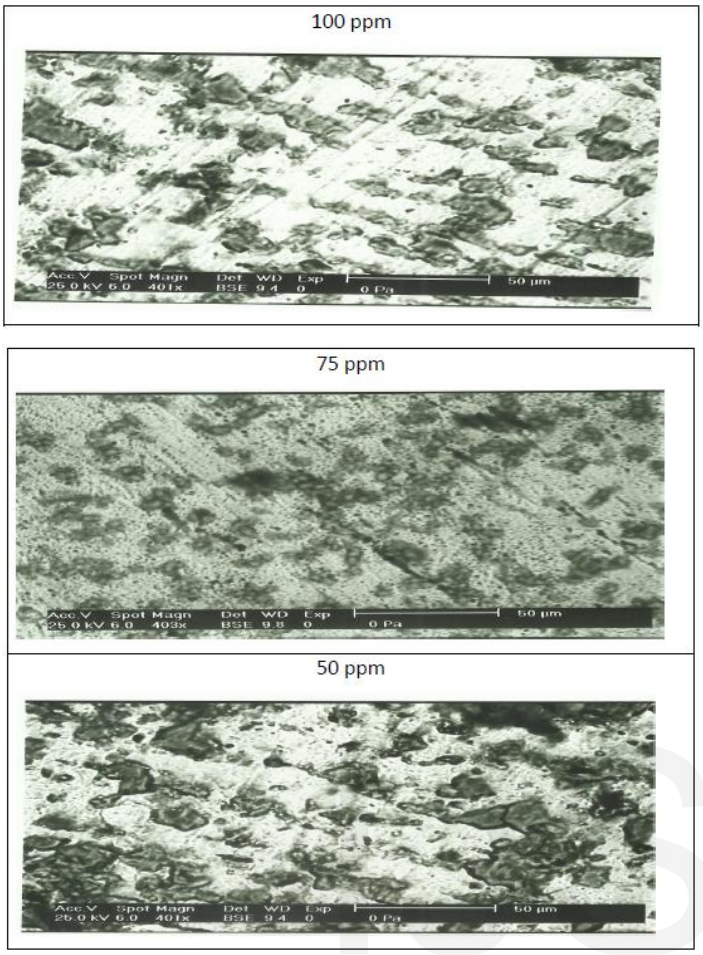

Fig. (8): SEM spectrum of C-steel before and after immersion for 15 h in 0.5M HCl solution without and with different concentrations of $Yb(NO_3)_3$

3. 6. Energy Dispersive X-ray (EDX) Analysis

The EDX spectra were used to determine the elements present on the surface of the carbon steel after 15 h of exposure to the uninhibited and inhibited 0.5 M HCl solution. Figs (9-10) shows the EDX analysis results on the composition of carbon steel with and without the inhibitor treatment in 0.5 M HCl solution, respectively. The EDX analysis indicates that only Fe and Cl were detected. The EDX analysis of carbon steel with the inhibitor treatment in 0.5 M HCl solution in the presence of different concentrations of $Yb(NO_3)_3$ and $Nd(NO_3)_3$ are shown in Figs. (9-10) respectively, the spectra show an additional line, demonstrating the existence of Yb and Nd and the height of this line increases by increasing the concentration of $Yb(NO_3)_3$ and $Nd(NO_3)_3$. This Figure show the presence of peaks related to Nd and Yb, this revealed the presence of a protective film of lanthanides on carbon steel surface. The height of the peak increases as follows: $Nd(NO_3)_3$ < $Yb(NO_3)_3$ and this parallel to the order of inhibition efficiency of these lanthanides.

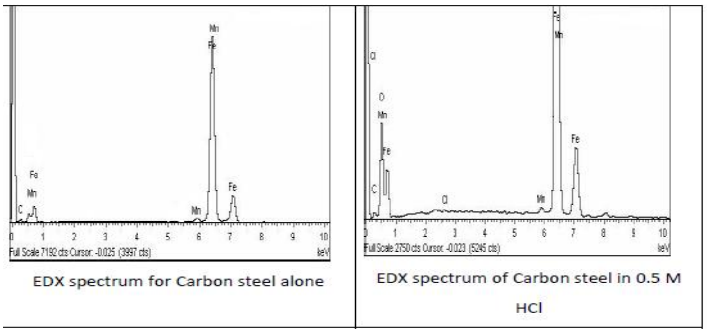

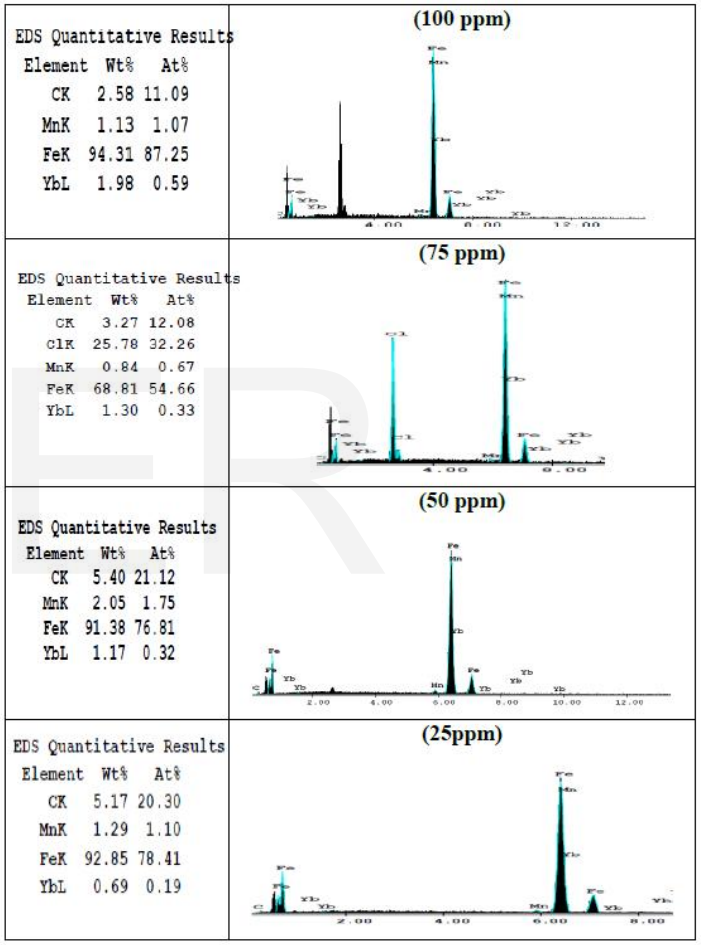

Fig. (9): EDX spectrum of carbon steel before and after immersion for 15 h in 0.5 M HCl solution without and with different concentrations of $Yb(NO_3)_3$.

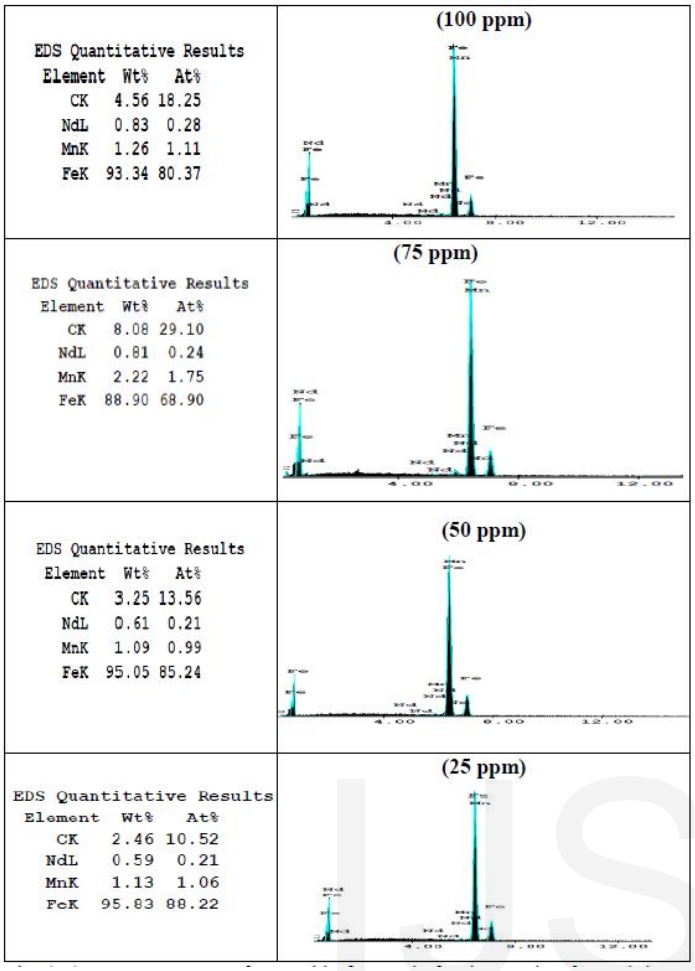

Fig. (10): EDX spectrum of C-steel before and after immersion for 15 h in 0.5 M HCl solution without and with different concentrations of $Nd(NO_3)_3$

4. Mechanism of Inhibition

Corrosion inhibition of carbon steel in 0.5 M hydrochloric acid solution by the investigated lanthanides compounds as indicated from potentiodynamic, electrochemical impedance spectroscopy (EIS), Electrochemical frequency modulation (EFM) and surface examinations (SEM and EDX) was found to depend on the concentration and the nature of lanthanide compounds. C-arbon steel is generally, assumed that adsorption of the inhibitor at the metal / solution interface is the first step in the action mechanism of the inhibitors in aggressive acidic solutions. Four types of adsorption may take place during inhibition involving lanthanide molecules at the metal/solution interface; (i) electrostatic attraction between charged molecules and charged metals, (ii) interaction of electron pairs in the oxygen and/or nitrogen with the metal, (iii) interaction of Л-electrons with the metals, and (iv) a combination of the above [51]. Concerning inhibitors, the inhibition efficiency depends on several factors; such as the number of adsorption sites and their charge density, molecular size, heat of hydrogenation, mode of interaction with the metal surface, and the formation metallic complexes [52]. The obtained results by potentiodynamic polarization, electrochemical impedance spectroscopy (EIS) and EFM techniques indicate that the extent of inhibition of lanthanides for corrosion of carbon steel in 0.5 M of HCl solutions obeys the following order: $Yb(NO_3)_3 > Nd(NO_3)_3$. The inhibition efficiency values can be explained on the basis of formation of lanthanide oxides or hydroxides over cathodic sites. Blocking of cathodic sites by these oxides or hydroxides, decreases the available cathodic current and, therefore, reduces the principal corrosion process of carbon steel. This explanation is supported by the results of several authors [53]. The explanation of the precipitation mechanism of rare earth oxides and hydroxides is based on the hydrolysis reactions experienced by the rare earth cations as proposed by Baes and Mesmer [54].

$$xMy^{+} + yH_2O \rightarrow Mx(OH)y(xy-y) + yH^{+} \quad (12)$$

As the product of this reaction, a complex hydroxylate is obtained whose stoichiometry depends on the pH of the solution, so that the higher the pH, the more favored is the precipitation of $Ln(OH)_3$:

$$Ln^{3+} + 3H_2O \rightarrow Ln(OH)_3 + 3H^{+} \quad (13)$$

The rare earth hydroxides formed do not possess amphoteric properties; they are stable in alkali solutions and dissolve in acid solutions. Consequently, the hydroxides will precipitate in those areas where pH is sufficiently alkaline to reach their solubility product. The rate of formation of $Ln(OH)_3$ is decreased in the following order: $Yb(OH)_3 > Nd(OH)_3$, which is parallel to their inhibition efficiency.

Supposing that the neodymium and ytterbium cations hydrolyze to precipitate the species $Ln(OH)_3$, it is possible to calculate the critical pH at which their precipitation occurs. These pH values are lower than theoretical pH that was calculated, which was reached on the cathodic areas, and therefore, the precipitation of the rare earth hydroxides is thermodynamically favorable, whether it occurs with an exchange of two or four electrons. For the same pH value, a greater concentration of [Ln3+] is needed for $Nd(OH)_3$ to precipitate than $Yb(OH)_3$ to precipitate. So, at the same pH the rate of formation of $Ln(OH)_3$ is decreased in the following order: $Yb(OH)_3$> $Nd(OH)_3$, which is parallel to their inhibition efficiency.

TABLE 8

PH VALUES FROM YB AND ND SOLUTIONS ACCORDING TO THE DIFFERENT CONCENTRATIONS

[inh.] ppm	pH	
	$Yb(NO_3)_3$	$Nd(NO_3)_3$
25	0.62	0.60
50	0.64	0.62
75	0.72	0.64
100	0.92	0.73

5. CONCLUSION

The corrosion studies of the carbon steel were carried out at room temperature using 0.5 M HCl, and the results indicated that lanthanides are effective corrosion inhibitor for Carbon steel in 0.5 M HCl. The studied inhibitors were observed to act as a mixed-type inhibitor, and EIS measurements clarified that the corrosion process was mainly controlled by charge transfer, and that no change in the corrosion mechanism occurred owing to the addition of inhibitor in 0.5 M HCl. The values of Rct increased with the addition of inhibitor, while the capacitance values decreased, indicating the formation of a surface film. The surface study (by SEM) indicated the formation of thin film on the iron specimen immersed in seawater containing the lanthanides.

REFERENCES

[1] T. J. Haley, Effect of surface preparation prior to cerium pretreatment, J. Pharm. Sci. 54 (1965) 633.
[2] P. J. Falconnet, The rare earth industry: a world of rapid change, J. Alloys Comp. 192 (1993) 114.
[3] S. R. Taylor, Abundance of chemical elements in the continental crust: A new table, Geochim. Cosmochim. Acta 28 (1964)1273.
[4] B. R.W, Hinton, L. Wilson, The corrosion inhibition of zinc 40 with cerous chloride, Corros. Sci. 29 (1989) 97.
[5] N. Verma, W.R. Singh, S.K. Tiwari, R.N. Singh, Influence of minor additions of La, Ce and Nd on the corrosion behavior of aluminum bronze in sulphuric acid solution, Br. Corros. J. 25 (1990) 131.
[6] F. Czrewinski, W. W. Smeltzer, Oxidation of metals, Lanthanide compounds as environmentally-friendly corrosion inhibitors of aluminum alloys: a review 40 (1993) 503.
[7] H. S. Isaacs, A. J. Davenport, A. Shipley, Electrochemical response of steel to the presence of dissolved cerium, J. Elect- 50 rochem. Soc. 138 (1991) 390.
[8] S. K. Mitra, S. K. Roy, S. K. Bose, Influence of superficial coating of CeO2 on the oxidation behavior of AISI 304 stainless steel, Oxidation Metals 39 (1993) 221.
[9] S. Bernal, F. J. Botana, J. J. Calvino, M. A. Cauqui, M. Marcos, 55 J.A. Perez, H. Vidal, in Proc. Lanthanide compounds as environmentally-friendly corrosion, Reunion Nac.de Materials, Oviedo, (1993), 258.
[10] S. Bernal, F. J. Botana, J. J. Calvino, M. A. Cauqui, M. Marcos, J. A. Perez, H. Vidal, in: Proc. Lanthanide compounds as 60 environmentally-friendly corrosion inhibitors, Visualizer-Untitled 13th Int. Conf. Electron Microscopy, Parts, Francia, (1994), 1105.
[11] S. Bernal, F. J. Botana, J. J. Calvino, M A. Cauqui, M. Marcos, J. A. Perez, H. Vidal, Lanthanide compounds as environmentally-friendly corrosion inhibitors, in: Proc. 2nd Int. Conf. on Elements, Helsinkii, Finlandia, (1994), 354.
[12] S. Bernal, F. J. Botana, J. J. Calvino, M. A. Cauqui, M. Marcos, J. A. Perez, Lanthanid compounds as environmentally-friendly corrosion inhibitors, in: Proc. 5th Elect. Methods in Corros. Research, Sesimbra, Portugal, (1994) 10.
[13] Y. C. Lu, M. B. Ives, Chemical treatment with cerium to improve the crevice corrosion resistance of austenitic stainless steels, Corros. Sci. 37 (1995) 145.
[14] S. Bernal, F. J. Botana, J. J. Calvino, M. A. Cauqui, M. Marcos, J. A. Perez, H. Vidal, Lanthanide salts as alternative corrosion inhibitors, J. Alloys Comp. 225 (1995) 638.
[15] K. Al-Muhanna, Corrosion behavior of different stainless steel alloys exposed to flowing fresh seawater by electrochemical impedance spectroscopy, Desalin. Water Treat. 29 (2011) 227.
[16] N. Larche, P. Dezerville, Review of material selection and corrosion in seawater reverse osmosis desalination plants, Desalin. Water Treat. 31 (2011) 121.
[17] A. U. Malik, I. Andijani, M. Mobin, S. Al-Fozan, F. Al-Muaili, M. Al-Hajiri, An overview of the localized corrosion problems—some recent case studies, Desalin. Water Treat. 20(2011) 22.
[18] R. W. Bosch, J. Hubrecht, W. F. Bogaerts, B. C. Syrett, Corrosion 57 (2001) 60.
[19] S. S. Abdel–Rehim, K. F. Khaled, N. S. Abd–Elshafi, Electrochim. Acta 51 (2006) 3269.
[20] E. Stupnisek-Lisac, A. Gazivoda and M. Madzarac, J. Electrochim.Acta, 47 (2002) 4189.
[21] G. N. Mu, X. H. L and Q. Quand J. Zhou, Corros. Sci., 48 (2006) 445.
[22] Sinyashin, Corros. Sci. 53 (2011) 976.
[23] V. V. Torres, R. S. Amado, C. F. de Sá, T. L. Femandez, C. A. Da Silva Riehl, A. G. Torres, E. D'Elia, J. Corros. Sci. 53 (2011) 2385.
[24] T. P. Zhao, G. N. Mu, Corros. Sci. 41 (1999)1937.
[25] M. J. Bahrami, S. M. A. Hosseini, P. Pilvar, J. Corros. Sci. 52 (2010) 2793.
[26] I. B. Obot, N. O. Obi-Egbed, J. Appl. Electrochem. 40 (2010) 1977–1984.
[27] A. Ostovari, S. M. Hoseinieh, M. Peikari, S. R. Shadizadeh, S. J. Hashemi, Croros. Sci. 51 (2009) 1935–1949.
[28] M. Bouklah, B. Hammouti, M. Lagrenée, F. Bentiss, Corros. Sci. 48 (2006) 2831.
[29] F. M. Donahue, K. Nobe, J. Electrochem. Soc. 112 (1965)886.
[30] E. Kamis, F. Bellucci, R. M. Latanision, E. S. H. El-Ashry, Corrosion 47(1991) 677.
[31] X. H. Li, S.D. Deng, H. Fu, G. N. Mu, Corros. Sci. 52 (2010) 1167.
[32] G. K. Gomma and M. H. Wahdan, Mater. Chem. Phys., 39 (1995).
[33] J. Marsh, Advanced Organic Chemistry, 3rd ed., Wiley Eastern New Delhi, (1988).
[34] M. S. Soliman, Ph. D. Thesis, Alex. Univ., Egypt (1995).
[35] M. Abdallah, Corros. Sci., 45 (2003) 2705.
[36] A. S. Fouda, A. A. Al-Sarawy and E. E. El-Katori, Desalination, 201(2006) 1.
[37] X. H. Li, S. D. Deng, H. Fu, G.N. Mu, Corros. Sci. 52 (2010) 1167.
[38] X. H. Li, S.D. Deng, H. Fu, G. N. Mu, Corros. Sci. 50 (2008) 2635.
[39] A. Döner, G. Kardas, N-Aminorhodanine Corros. Sci. 53 (2011) 4223.
[40] G. Moretti, G. Quartarone, A. Tassan, A. Zingales, J. Werkst. Korros. 45 (1994) 641.
[41] B. G. Ateya, B. E. El-Anadouli, F. M. El-Nizamv, Corros. Sci. 24 (1984) 509.
[42] F. H. Assaf, M. Abou-Krish, A. S. El-Shahawy, M. Th. Makhlouf, Hala Soudy, Int. J. Electrochem. Sci. 2 (2007) 169.
[43] I. Sekine, M. Sabongi, H. Hagiuda, T. Oshibe, M. Yuasa, T. Imahc, Y. Shibata, and T. Wake; J. Electrochem. Soc.; 139 (1992) 3167.
[44] L. Larabi, O. Benali, S. M. Mekelleche and Y. Harek, Appl. Surf. Sci., 253 (2006) 1371.
[45] M. Lagrenee, B. Mernari, B. Bouanis, M. Traisnel and F. Bentiss, Corros. Sci., 44 (2002) 573.
[46] G. A. Caigman, S. K. Metcalf, E. M. Holt, J. Chem. Cryst.30 (2000) 415.
[47] D. C. Silverman and J. E. Carrico, National Association of Corrosion Engineers, 44 (1988), 280.
[48] R. A., Prabhu, T. V., Venkatesha, A. V., Shanbhag, G.M., Kulkarni, R.G., Kalkhambkar, Corros. Sci., 50 (2008) 3356.

[49] R. A., Prabhu, T. V., Venkatesha, A. V., Shanbhag, G. M., Kulkarni, R. G., Kalkhambkar, Corros. Sci., 50 (2008) 3356
[50] G., Moretti, G., Quartanone, A., Tassan, A., Zingales, Wekst. Korros., 45 (1994) 641.
[51] F. Mansfeld and Y. Wang, Br. Corros. J., 29 (1994) 194.
[52] F. Mansfeld and Y. Wang and H. Shih, J. Electrochem. Soc., 138 (1991) 174.
[53] A. J. Aldekiewicz, H.S. Isaacs and A.J. Davenport, J. Electrochem. Soc., 142 (1995) 3342.
[54] C. F. Baes, R.E. Mesmer, Hydrolysis of Cations, John Wily and Sons, N. Y., (1976).